

Investigation of Interface Diffusion in Sputter Deposited $Gd_{0.1}Ce_{0.9}O_{1.95}$ Thin Buffer Layers on Y-Stabilized Zirconia Crystalline Substrates for Solid Oxide Cells Applications

Nunzia Coppola¹, Giovanni Carapella², Chiara Sacco¹, Pasquale Orgiani³, Alice Galdi⁴, Pierpaolo Polverino⁵, Alberto Ubaldini³, Luigi Maritato^{1*} and Cesare Pianese⁵

¹Dipartimento di Ingegneria Industriale-DIIN, Università di Salerno and CNR-SPIN, Fisciano, (SA), Italy

²Dipartimento di Fisica "E.R. Caianiello", Università degli Studi di Salerno, and CNR-SPIN, Fisciano, (SA), Italy

³CNR SPIN U.O.S. Salerno, Fisciano (SA), Italy

⁴CLASSE, Cornell University, Ithaca (NY), USA

⁵Dipartimento di Ingegneria Industriale-DIIN, Università di Salerno, Fisciano, (SA), Italy

Abstract

This paper presents the results concerning the investigation of the morphological and structural properties of $Gd_{0.1}Ce_{0.9}O_{1.95}$ layers deposited on crystalline (111) YSZ substrates by RF magnetron sputtering. Room temperature as-grown samples have been annealed at different temperatures from 600°C to 1300°C. Atomic Force Microscopy analysis shows an increase in the average grain size dimensions with increasing annealing temperatures. X-Ray Diffraction measurements indicates a preferential growth of the grains along the (111) direction with a decrease in the evaluated c-axis as a function of the annealing temperature, probably related to an over-oxidation of the samples. X-Ray Reflectivity studies, performed on thin layers annealed at temperatures from 700-1000°C, points out the presence of zones with different densities and roughness at the layer/substrate interface and at the layer/vacuum surface. The behaviour of these zones as a function of temperature has been investigated. The obtained results seem to exclude the presence of consistent inter-diffusion phenomena at the GDC/YSZ interface.

Keywords: Gadolinium doped Ceria; Yttrium stabilized Zirconia; X-ray reflectivity; RF magnetron sputtering; Interdiffusion; Reciprocal space map; Solid oxide cells

Introduction

Recent advancements in materials research for solid oxide fuel cells (SOFC) have been driven by the need for reduced costs and increased durability. Both these goals can be achieved by decreasing the operating temperature of SOFC to the so-called intermediate temperature (IT) range (500-700°C) [1,2]. The use of such an IT range calls for new cell materials and design [3]. For example, in IT-SOFC, conventional La,Sr-Manganite (LSM) cathodes are generally replaced by La,Sr-Cobaltite (LSC) cathodes to reduce the cell polarization resistance at low temperatures [4] and this substitution causes the formation of low conductivity unwanted phases at the LSC/Electrolyte interface during the sintering process [5]. To reduce such an interface diffusion, the introduction of a Gadolinium doped Ceria (GDC) buffer layer at the cathode/electrolyte interface has been proposed. In this case, due to the formation of spurious solid solutions at the GDC/YSZ interface for temperatures higher than 1000°C, the use of suitable deposition techniques is required [6]. Physical Vapour Deposition (PVD) techniques generally do not involve temperatures higher than 700-800°C for GDC layers production, and, when compared to standard ceramic processes, they allow to obtain much smaller layer thicknesses with higher density.

In the last years, several PVD techniques have been investigated aiming at finding a suitable GDC buffer layers production process to be implemented in the industrial fabrication of IT-SOFC. For example, Wang et al. [7] studied the microstructure of ZrO_2 - CeO_2 hetero-multi-layer films grown by oxygen plasma assisted molecular beam epitaxy on single crystal (111) YSZ substrates, finding that the film growth process introduced the displacement of the oxygen ions from the ideal fluorite position. Shi et al. [8] investigated the influence of the deposition atmosphere on the properties of CeO_2 thin films grown by Pulsed Laser Deposition (PLD) on (100) YSZ single crystal substrates.

Wu et al. [9] analysed the morphology of CeO_2 thin layers deposited by electron beam evaporation on (100), (111) and (110) YSZ single crystal substrates obtaining the best results in terms of surface flatness in the case of (111) YSZ substrates. Song et al. [10] studied the reduction of Ce^{4+} to Ce^{3+} in CeO_2 thin films deposited by PLD on (111) oriented YSZ crystalline substrates.

All the studies previously addressed dealt with small area single crystal YSZ substrates to focus on material science aspects related to the diffusion mechanisms at the GDC/YSZ interface, in order to analyse the investigated detrimental processes and point out their dependence on the specific used PVD technique. However, approaching industrial processes, the production of SOFC involves large area polycrystalline substrates, rather than single crystals. Among the various PVD techniques, sputtering represents the most promising one for large scale industrial applications, being already used in several coating sectors [11].

Several works showed that the sputtering technique is able to produce thin dense GDC buffer layers on polycrystalline YSZ substrates with Area Specific resistance (ASR) down to $0.27 \Omega cm^2$ [12,13]. Nevertheless, from the available scientific literature, the analysis of the interdiffusion phenomena at the sputter deposited GDC/YSZ interface in the case of

*Corresponding author: Luigi Maritato, Dipartimento di Ingegneria Industriale-DIIN, Università di Salerno and CNR-SPIN, Fisciano, (SA), Italy, Tel: +39 089 96 8202; E-mail: lmaritato@unisa.it

Received August 28, 2018; Accepted September 12, 2018; Published September 22, 2018

Citation: Coppola N, Carapella G, Sacco C, Orgiani P, Galdi A, et al. (2018) Investigation of Interface Diffusion in Sputter Deposited $Gd_{0.1}Ce_{0.9}O_{1.95}$ Thin Buffer Layers on Y-Stabilized Zirconia Crystalline Substrates for Solid Oxide Cells Applications. J Material Sci Eng 7: 482. doi: 10.4172/2169-0022.1000482

Copyright: © 2018 Coppola N, et al. This is an open-access article distributed under the terms of the Creative Commons Attribution License, which permits unrestricted use, distribution, and reproduction in any medium, provided the original author and source are credited.

crystalline YSZ substrates seems not to be yet accomplished. Sputter deposited single crystal analysis is although essential to decouple intrinsic material properties from microstructure related effects and from the presence of secondary phases at the interfaces. Moreover, the study of the diffusion phenomena between the GDC sputter deposited buffer layer and the crystalline YSZ, as a function of the temperature at which the system is exposed, is fundamental to look for innovative production processes, able to improve the final performance of the cell.

This work illustrates the analysis of morphological, structural and interface diffusion properties of GDC buffer layers. The fabrication process involved GDC layers deposition on crystalline (111) YSZ substrates by RF sputtering starting from an oxide $Gd_{0.1}Ce_{0.9}O_{1.95}$ 6" target. The as-grown samples underwent an annealing treatment at different temperatures from 600°C to 1300°C. Their morphological and structural properties were investigated by Atomic Force Microscopy (AFM), X-Ray Diffraction (XRD) and X-Ray Reflectivity (XRR) measurements. Only non-destructive characterization techniques have been considered, due to the possibility to apply such techniques as standard on-line quality controls within industrial SOFC production processes. AFM analysis results show an increase in the average grain size dimensions with increasing annealing temperatures. XRD analysis indicates a preferential growth of the grains along the (111) direction with a decrease in the evaluated lattice parameter in the growth direction as a function of the annealing temperature, probably related to an over-oxidation of the sample. XRR measurements show the presence of zones with different densities and roughness at the layer/substrate interface and at the layer/vacuum surface. The behaviour of these zones, as a function of the temperature at which the system was exposed, has been also investigated.

Experimental Methods

GDC thin films have been deposited starting from a 6 inches oxide target ($Gd_{0.1}Ce_{0.9}O_{1.95}$, Testbourne 99.999% purity) on single crystal (111) (YSZ, 9.5 mol% Y_2O_3 , Crystec) with a lattice constant of 0.512 nm, measured RMS surface roughness of 0.8 nm and a miscut below 0.1° (as reported on Crystec YSZ substrates datasheet). RF Sputtering parameters were 400 W power applied at 13.5 MHz with an Ar (99.999% purity) pressure of 2.2 mTorr, starting with base pressure of 5×10^{-4} mTorr. Sputtering deposition times are 10 minutes for the thick samples (around 300 nm thick) used for XRD and 1 minute for the thin samples (around 30 nm thick) used for XRR measurements. Preliminary XRR measurements were performed on different substrates (MgO , Al_2O_3 and YSZ) in order to determine the deposition rate and, moreover, to check if it was substrate dependent. XRR showed that the deposition rate is about 30 nm/min and, as expected, is independent from the particular substrate used: indeed one of the key points of the use of RF Sputtering technique is the well-established long time reproducibility of the method.

As grown 300 nm thick samples were annealed at different temperatures ranging from 600°C to 1300°C in a muffle furnace (in air atmosphere) with a heating ramp of 30°C/min; as the set temperature was reached, thin films were annealed for 2 hours and then quenched out.

X-Ray Reflectivity measurements have been performed using a Bruker D2 Phaser equipped with a Cu source ($\lambda=1.541 \text{ \AA}$) and a set angular resolution of about 0.002 2 θ degrees.

X-Ray Diffraction measurements have been performed using an XPert Pro PANalytical equipped with a Cu source ($\lambda=1.541 \text{ \AA}$) with

a set angular resolution of about 0.01 2 θ degrees. In this case the measurements were systematically performed on GDC thin films 300 nm thick deposited on YSZ crystalline substrates in order to acquire data on the crystal structure of the samples (c-axis and preferred orientation of the grains).

AFM measurements were performed using a Nanite AFM from Nanosurf in dynamic (tapping) mode in air [14,15]. The AFM head has 0.3 nm RMS Z resolution and 1.5 nm XY resolution.

Experimental Results and Discussion

Samples growth and morphological analysis

During the deposition process of the GDC thin buffer layers, the YSZ substrates were not heated and typically reached temperatures not higher than 100-150°C. Layers of about 300 nm thickness were deposited with a deposition rate of about 30 nm/min, as estimated by XRR measurements. As-grown samples underwent an annealing treatment at different temperatures ranging from 600°C to 1300°C in air atmosphere for 2 hours, in order to study possible temperature-induced changes in the structure of the thin buffer layers and at the GDC/YSZ interface.

The surface morphology of the deposited samples as a function of the annealing temperature was studied through AFM measurements. Typical AFM Z-axis scans over a $3\mu\text{m} \times 3\mu\text{m}$ surface area for a 300 nm thick sample are shown in Figure 1. Specifically, Figure 1a presents a sample immediately after the deposition process (as-grown), whereas Figure 1b shows the sample after the 2 hours annealing process in air atmosphere at 1300°C. The as-grown sample shows an estimated surface RMS roughness of 4 nm and an average grain size of 100 nm, while the annealed one presents a surface RMS roughness of 18 nm and an average grain size of 500 nm.

The increase in the average grain size with the annealing process implies a decrease in the grain boundary surface density and, consequently, a reduction of the grain boundary effects. However, the average grain size values, shown in Figure 1b, are lower than those usually observed in thick GDC buffer layers grown by standard (not PVD) techniques [13,16].

Crystal structure analysis

XRD measurements have been performed to i) check the achievement of the desired phase, ii) evaluate the possible presence of unwanted spurious phases and iii) make an overall structural characterization of the samples. Figure 2 shows the XRD spectra of an as-grown sample (blue line) and of a sample annealed for 2 hours in air atmosphere at 1200°C. Both the curves show the expected peak associated to the presence of the GDC phase grown with a preferential orientation along the (111) direction, which is also the orientation of the used YSZ crystalline substrates. This is a strong indication of the fact that GDC thin films sputter-deposited grow with one domain determined by the orientation of the single crystal substrate. The two arrows associated to the as-grown sample (blue line) highlight peaks probably related to unreacted spurious phases, which could have been induced by the presence of Gadolinium oxides as a result of the low substrate temperature during the deposition process. This hypothesis is confirmed by the disappearance of the spurious peaks in all the annealed samples (i.e., magenta line). Moreover, the sharpening of the (111) peak going from the as-grown to the annealed sample, confirms the results of the AFM measurements, with the increase in the average grain size dimension at higher annealing temperatures.

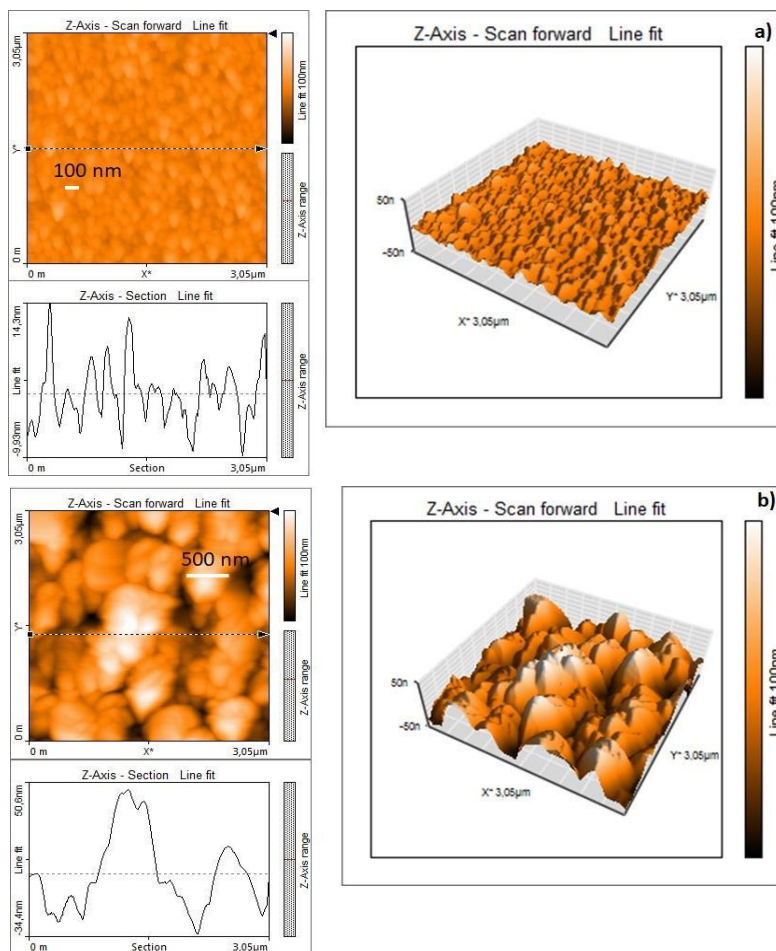


Figure 1: a) AFM image of an as-grown GDC layer (300 nm thick) showing an estimated surface RMS roughness of 4 nm and medium grain size of 100 nm; b) AFM image of the same GDC layer (300 nm thick) after an annealing process of 2 hours in air atmosphere at 1300°C, presenting a surface RMS roughness of 18 nm and a medium grain size of 500 nm.

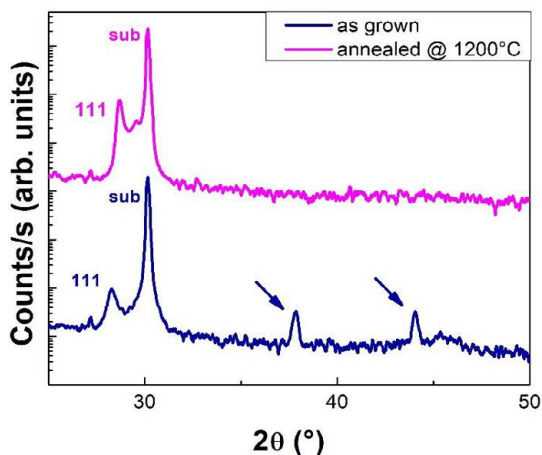


Figure 2: XRD spectrum of an as-grown sample (blue line) and of a sample annealed at 1200°C in air atmosphere for 2 hours (magenta line). GDC and YSZ substrate contributions are indicated for both the samples and blue arrows point out peaks related to the formation of some spurious phases in the as-grown sample that disappear after annealing. The two curves have been vertically shifted for clarity.

When compared to those grown by Arndt et al. [17], which deposit by Pulsed Laser Deposition (PLD) epitaxial GDC thin films on YSZ (110) and (111) oriented single crystal substrates heated, during the grow, at a temperature of 925 K, our GDC films are rather polycrystalline with a preferred (111) orientation of the grains induced by the substrates. This is not surprising because we have deposited our GDC films without heating the substrates above temperatures of 100-150°C. As shown by our XRD results, the crystallinity of the samples was greatly improved after the 2 hours annealing process in air.

The plot on the left side of Figure 3 shows XRD measurements performed on a series of 9 samples, going from the as-grown sample to those annealed for 2 hours in air atmosphere at different temperatures ranging from 600°C to 1300°C. The average increase in the (111) peak intensity with increasing annealing temperatures is probably due to the growth in the average grain size already outlined by the AFM measurements and confirmed by the Debye-Scherrer formula [18] applied to the (111) peak. Moreover, the data show a tendency of the 2θ degree angles at which the (111) peak is observed to move toward higher values with increasing annealing temperatures.

The crystal axis parameter values along the growth direction (c-axis) of the deposited GDC layers have been evaluated from the 2θ degree angles at which the (111) peak is observed. It can be seen that

the c-axis values are smaller than the bulk value for GDC found in the literature (e.g., 5.412 Å [19]). Arndt et al. [17] observe an increase in the lattice parameter of their samples after a reducing (ultra-high vacuum conditions) post growth annealing at high temperature (1400 K). Our sputter deposited GDC thin films show, on the contrary, a compression of c-axis parameter as they were annealed in an oxidizing atmosphere (ambient pressure air). This result can be generally ascribed to two different mechanisms: i) strain effects induced in the GDC crystal structure by the different in-plane crystal parameters between the YSZ substrate and the GDC buffer layer; ii) over-oxidation with the related change in the electropositive ions ratios, induced in the samples during the annealing process in air [20-22].

Typically, high temperature processes work against substrate-induced strain effects promoting their release while they enhance the inclusion of extra oxygen in the GDC structure. Therefore, the observed temperature-dependent behaviour of the GDC c-axis may indicate the possible presence of extra oxygen (or electropositive vacancies) in the sputter deposited buffer layers. To further prove the absence of strain effects in the GDC buffer layers, the measurement of the reciprocal space asymmetric map along the GDC (224) reflection peak on a sample annealed at 1300°C for 2 hours in air atmosphere has been performed (Figure 4). In this map, the peak related to the GDC

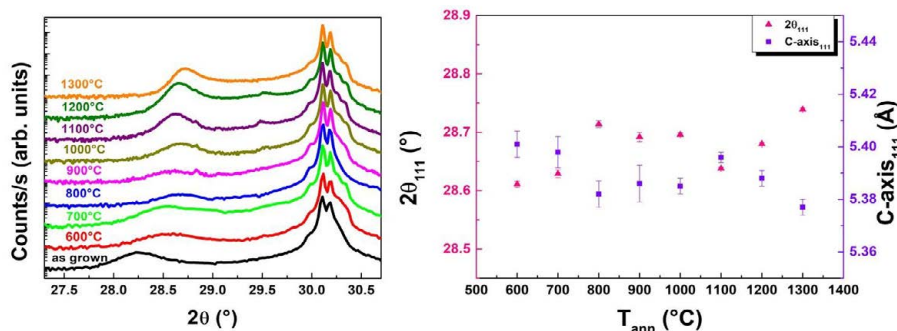


Figure 3: Left side: XRD performed in proximity of the (111) reflection peak for samples annealed at different temperatures; the curves are vertically shifted for clarity. Right side: plot of the $2\theta_{111}$ peak angular position and of the evaluated c-axis as function of the annealing temperature.

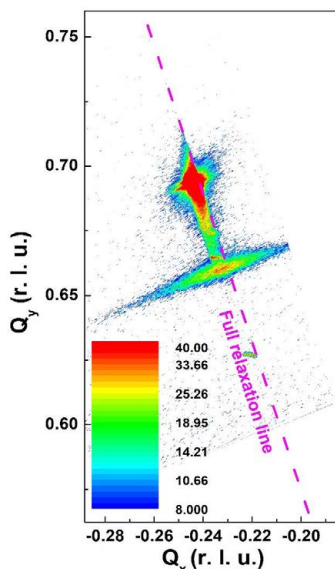


Figure 4: reciprocal space map along the (224) direction on a sample annealed at 1300°C for 2 hours in air atmosphere.

buffer layer is shifted on the left side of the full relaxation line, clearly indicating that the GDC layer is relaxed and does not present any sign of YSZ substrate induced strain effect. The decrease of the GDC c-axis with increasing annealing temperatures should be, therefore, traced back to over-oxidation of the thin GDC buffer layers. It is worth noting that sputtering deposition is a metastable process, which allows in the produced samples the emerging of states that are often more difficult (or even impossible) to obtain in the bulk material.

From Figure 4, the values of the projection of the in-plane Q_x and out-of-plane Q_y vectors in the reciprocal space, for both the GDC layer and the YSZ substrate, have been also computed, obtaining $Q_x(YSZ)=0.24568$, $Q_x(GDC)=0.23247$ and $Q_y(YSZ)=0.6948$, $Q_y(GDC)=0.6575$, respectively. From these values we can calculate the ratios between the out-of-plane and in-plane projections of GDC and YSZ, in order to compare their crystal structures. If the GDC thin film grows with a cubic structure on the cubic YSZ substrate, both structures are expected to be characterized by one lattice parameter only, i.e. $a=b=c$, and, hence, all the evaluated d-spacings and their projection along the Q_x and Q_y directions should have the same proportionality factor. In the case of bulk YSZ and GDC, since they both grow with a cubic structure, it is obtained the following ratio:

$$\left(\frac{Q_{x=y}(YSZ)}{Q_{x=y}(GDC)}\right)^{-1} = \left(\frac{5.12\text{\AA}}{5.41\text{\AA}}\right)^{-1} = 0.9464$$

For the samples considered in the present work, both in plane and out-of-plane ratios can be evaluated as:

$$\left(\frac{Q_x(YSZ)}{Q_x(GDC)}\right)^{-1} = 0.9463 \text{ (in-plane)}$$

$$\left(\frac{Q_y(YSZ)}{Q_y(GDC)}\right)^{-1} = 0.9462 \text{ (out-of-plane)}$$

The two results show that the in-plane and out-of-plane projections “scale” as the bulk cubic lattice parameters, independently from the used reflection. This is a strong indication of the cubic growth of the GDC layer on the (111) YSZ substrate. Moreover, as shown in Figure 5, phi-scan measurements have been carried out. These measurements present a tight alignment between layer and substrate peaks which confirmed the growth of GDC on YSZ with the same crystal structure.

X-Ray reflectivity (XRR) measurements

XRR technique allows to obtain information about the eventual presence of extra layers in the deposited films along with their thickness, roughness and density [17]. XRR measurements have been performed depositing 30 nm thick (1 minute deposition time) GDC samples, which have been then annealed in air for 2 hours at 700°C, 800°C, 900°C and 1000°C. The results of the XRR measurements are shown in Figure 6. Changes in curves shape as function of the annealing temperatures are evident. In particular, as the temperature increases, the intensity of the oscillations decreases and this effect is eventually associated to the presence of increasing inter-diffusion in the investigated samples [23]. An accurate analysis of these inter-diffusion phenomena is crucial since they can contribute to downgrade the cell material at high working temperatures and thus lower the performance of the cell with time. To deeply investigate the dynamics of the inter-diffusion phenomena as a function of the annealing temperature, the XRR curves in Figure 6a have been fitted by means of routine based on the Parratt recursion formula [24,25], presented in Figure 6b.

In agreement to previous results [17], the best fitting curve is always obtained considering the GDC buffer layer composed of three different zones, as schematically sketched in Figure 7a, using the thickness, density and roughness of each zone as free fitting parameters.

In Table 1, the results of the fitting procedure are presented in detail for all the investigated annealing temperatures from 700°C to 1000°C. The roughness values of Zone III at all the annealing temperatures are always below 11 Å, comparable to the value of the as-grown sample (17 Å). This is a first indication that, in the investigated temperature range, no temperature-promoted inter-diffusion phenomena seem to take place at the GDC/YSZ interface besides those related to the deposition process.

The data in the Electron Density Profile (EDP) column in Tables 1 and 2, are the number of scatterers per unit volume in \AA^3 [26], given in $(u/\text{\AA}^3)$ where u is the relative atomic mass ($1u=1.66054 \times 10^{-27}\text{Kg}$). Therefore, having

$$(\text{kg/m}^3)=1.66054 \times 10^3 \times (u/\text{\AA}^3) \quad (1)$$

the EDP values are related to the $\rho(\text{kg/m}^3)$ densities via the formula $\text{EDP}=(\text{kg/m}^3)/(1.66054 \times 10^3 \times f) \quad (2)$

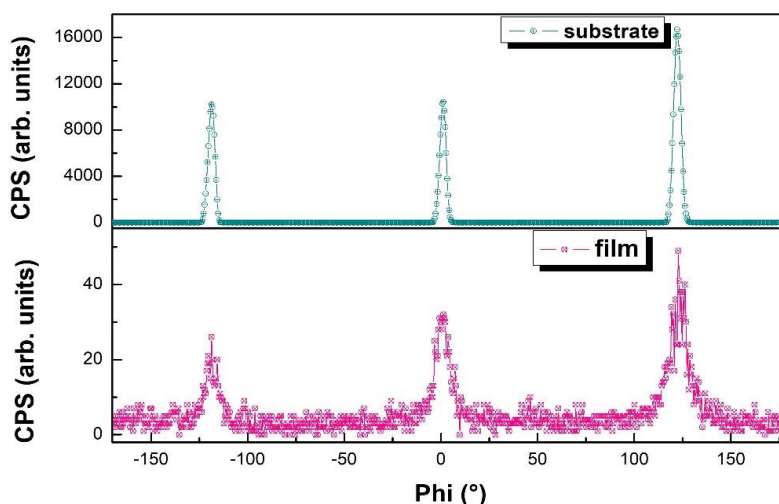


Figure 5: Phi-scan of a sample annealed at 1300°C, showing a perfect alignment of the peaks due to the GDC film (magenta line) and the substrate (green line).

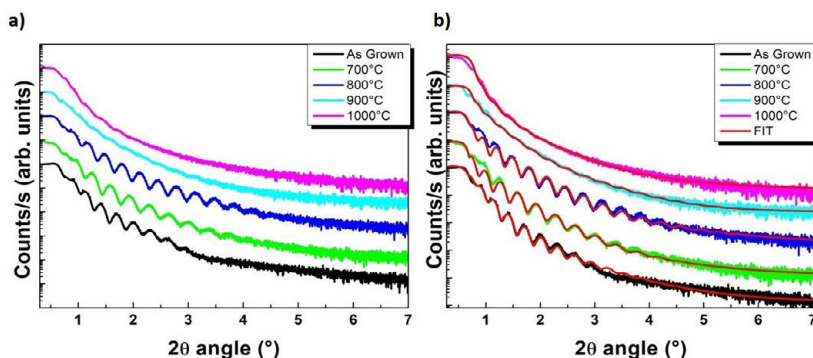


Figure 6: a) XRR measurements of the 30 nm thick GDC layer as-grown and annealed at different temperatures (the curves are vertically shift for clarity); b) same curves with best fitting curves superposition (red lines).

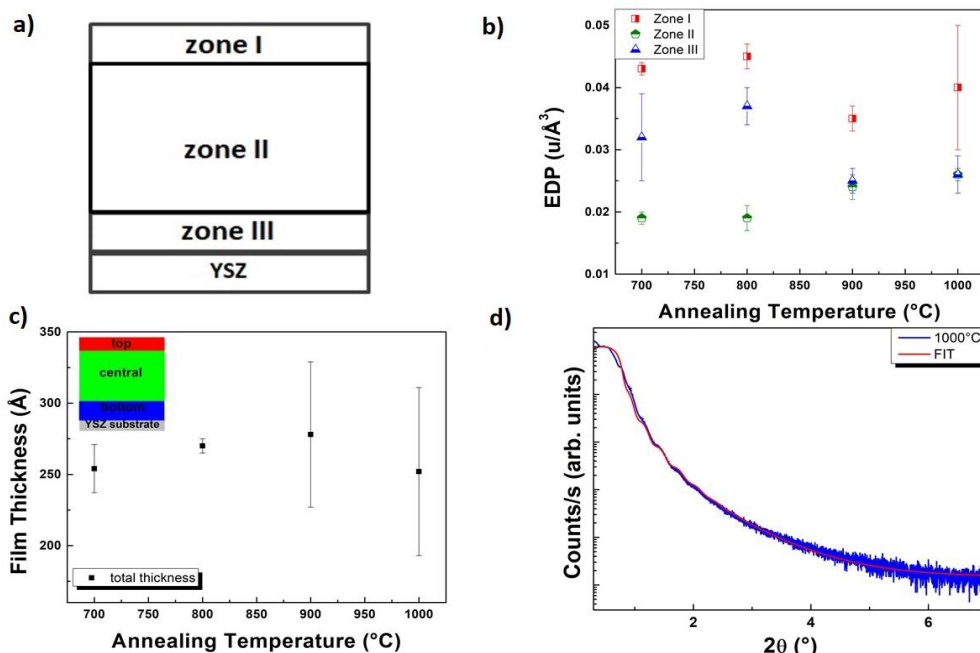


Figure 7: a) Schematic representation of the three zones of the GDC thin film grown on crystalline YSZ. Zone I is in contact with the atmosphere, Zone II is associated to the GDC buffer layer and Zone III is in contact with the YSZ substrate; b) EDP values evaluated from the fitting process for each of the three zones at different annealing temperatures; c) Total film thickness evaluated as the sum of the three zones thicknesses; d) XRR measurements for the sample annealed at 1000°C. The superposed red line is the curve obtained from the fitting routine performed considering the GDC film composed by two zones.

with

$$f = \sum u_i \times x_i \quad (3)$$

where the sum is performed over the number of atomic species present in the chemical formula unit, x_i is the relative concentration of the species and u_i is directly related to the atomic mass of the species. In the case of $Gd_{0.1}Ce_{0.9}O_{1.95}$, for example, with a bulk density of 7.2 g/cm³ [27], we have

$$f = 0.1 \times 157.25 + 0.9 \times 140.12 + 1.95 \times 16 = 173.03$$

giving

$$EDP(GDC) = 7.2 \times 10^3 / (1.66054 \times 10^3 \times 173.03) = 0.025.$$

The obtained EDP values of the bottom zone (Zone III) decrease with increasing annealing temperatures, reaching, at temperatures

around 900°C, a value very close to the one expected in the case of bulk $Gd_{0.1}Ce_{0.9}O_{1.95}$. This behaviour is in agreement with the XRD results, showing peaks of spurious phases disappearing with increasing temperatures. It is reasonable to assume that these phases are partially formed at the GDC/YSZ interface during the deposition and that the annealing process remove them, promoting reactions to form the GDC phase. This hypothesis is also confirmed by the temperature behaviour of the EDP values of the central zone (Zone II). At low annealing temperatures (up to 800°C) the Zone II values are slightly lower from the expected bulk value, while they reach values very close to the one expected for bulk GDC for higher temperatures (900-1000°C). For a better comparison of the temperature behaviours of the EDP values of all the three zones, they are shown as a function of the annealing temperature in Figure 7b. The EDP values of the top layer (Zone I) are always higher than the value expected for bulk GDC. Previous

Temperature	Layer	Thickness (Å)	Electron Density Profile($u/\text{Å}^3$)	Roughness (Å)
As Grown	Zone III	16 ± 8	0.032 ± 0.007	17 ± 2
	Zone II	264 ± 2	0.019 ± 0.001	2.5 ± 0.1
	Zone I	19 ± 6	0.043 ± 0.001	34 ± 9
700°C	Zone III	14 ± 17	0.038 ± 0.005	9 ± 1
	Zone II	224.9 ± 2.7	0.019 ± 0.004	1.8 ± 0.3
	Zone I	15.7 ± 1.9	0.042 ± 0.001	10.7 ± 1.1
800°C	Zone III	10 ± 3	0.037 ± 0.003	7 ± 2
	Zone II	244 ± 3	0.019 ± 0.002	0.4 ± 0.4
	Zone I	16 ± 2	0.045 ± 0.002	11 ± 1
900°C	Zone III	20 ± 20	0.025 ± 0.002	4 ± 1
	Zone II	229 ± 47	0.024 ± 0.002	15 ± 1
	Zone I	28 ± 4	0.035 ± 0.002	3.2 ± 0.2
1000°C	Zone III	5 ± 20	0.026 ± 0.003	11 ± 1
	Zone II	236 ± 55	0.026 ± 0.001	0.5 ± 0.4
	Zone I	11 ± 1	0.04 ± 0.01	11.2 ± 1.1

Table 1: Parameter values obtained from the fitting procedure. Substrate roughness has been maintained fixed at 0.8 nm as estimated from AFM measurements.

Temperature	Layer	Thickness (Å)	Electron Density Profile($u/\text{Å}^3$)	Roughness (Å)
900°C	GDC (ZoneII+Zone III)	265 ± 32	0.030 ± 0.003	1.9 ± 1.3
	Top	13.3 ± 1.9	0.040 ± 0.002	5.9 ± 0.5
1000°C	GDC (ZoneII+ZoneIII)	247 ± 34	0.026 ± 0.001	1.9 ± 0.1
	Top	6.5 ± 1.3	0.040 ± 0.001	6.11 ± 1.05

Table 2: Parameter values obtained from the fitting procedure. Substrate roughness has been maintained fixed at 0.8 nm as estimated from AFM measurements.

XRR results on GDC buffer layers deposited by Pulsed Laser on YSZ crystalline substrates [17], showed the presence of a very thin top zone with EDP values lower than those observed in the central zone (Zone II) and this observation was related to the possible surface adsorption of light molecules, such as water. It is worth remarking that, see formula (2), changes in the EDP values are related to variations in both the ρ (kg/m^3) and f and therefore, without having an alternative information on the layer composition, it is not possible to draw any conclusion about the kind of atomic species and compounds present in the investigated layer. Moreover, differently from the GDC buffer layers in a study [17], deposited at 925 K with an O_2 partial pressure of 0.04 mbar and then annealed in vacuum, the room-temperature sputtered samples analysed in this work have been annealed in air atmosphere for 2 hours at temperatures ranging from 700°C to 1000°C. Surface migration or pollution of elements during the exposure to atmospheric pressure and the annealing procedure can qualitatively explain the observed high EDP values of the top zone (Zone I). Further analysis about the stoichiometric composition of Zone I should be performed to confirm it. We point out that the small thickness of Zone I (always below 2 nm) poses severe problems to performing spectroscopic analysis able to give quantitative information on its stoichiometric composition.

The total thickness of the GDC buffer layer as a function of the temperature is shown in Figure 7c. Its value is almost constant and close to the expected one in terms of the deposition rate (26.8 nm/min). The error bars are obtained by the usual propagation of the errors associated to each single zone in Table 1. In the case of Zone I and Zone III, the obtained errors are quite high (around 100%) and this can be plausibly due to their very small thickness. Moreover, from the data in Table 1, it can be pointed out that the temperature of 900°C seems to give the best result in terms of the EDP values and the roughness of the different zones.

The equality between the EDP values of Zone III and those of Zone II for 900°C and 1000°C annealing temperatures (Table 1), suggests that, from 900°C, the GDC film can be considered as composed by only two zones, due to the merging of Zone II and Zone III. This is

also confirmed by the good accordance with the experimental curves obtained by fitting the curves considering only two zones, as shown in Figure 7d, for the sample annealed at 1000°C. In Table 2 the fitting parameters obtained with the two zones structure are shown as well. This result is a further indication that the appearance of a third zone at the GDC/YSZ interface is only dependent on the considered room temperature deposition-technique.

The combined AFM, XRD and XRR analyses performed on GDC layers sputter deposited at room temperature on YSZ crystalline substrates and then annealed in air at different temperatures point out the presence of three zones in the obtained samples and give indications of the role these zones play on the layer/substrate inter-diffusion properties. The picture emerging from our results is that of a layer/substrate interface showing (XRD measurements) the presence, in the case of as grown samples, of spurious/unreacted phases probably incorporated during the room temperature sputtering process, which almost completely disappear after the annealing procedure. As enlightened by the XRR analysis, at low annealing temperatures (700-800°C), this presence imply EDP values of the Zone III (the one at the layer/substrate interface) slightly larger than those expected in the case of bulk GDC. At higher annealing temperatures (900-1000°C), the EDP values of Zone III merge into those obtained for the central and thicker Zone II, giving a strong indication of the absence of important inter-diffusion process at the layer/substrate crystalline interface studied in this work. The very thin top zone (Zone I) shows constant values of thickness, EDP and roughness at different temperatures, and its presence is probably due to surface migration or pollution of elements during the exposure to atmospheric pressure and the annealing procedure.

Conclusions

GDC sputter deposited thin films have been studied from the point of view of morphology and crystal structure as a function of the annealing temperature in the range 700-1000°C, investigating the presence of eventual inter-diffusion phenomena at the GDC/YSZ

interface. AFM morphological analysis performed on 300 nm thick GDC buffer layers indicated an improvement of the layer crystallinity with increasing annealing temperatures associated to an increase in the average grain size. XRD measurement showed a preferential (111) growth direction coincident with the orientation of the YSZ substrate. Unreacted spurious phases, possibly related to Gadolinium oxides have been observed in the as grown sample disappearing in the annealed samples. A decrease in the obtained c-axis values with increasing annealing temperatures has been observed and, due to the absence of effects related to the substrate induced strain, has been tentatively associated to an over-oxidation and to a change in the electropositive ions ratio. XRR measurements, performed on 30 nm thick GDC layers, indicated the presence of a three-zones structure with a central zone showing EDP values in agreement with those expected for bulk GDC, a top zone with EDP values higher than those observed in the central zone probably due to film/atmosphere interaction and a bottom zone at the GDC/YSZ interface presenting high temperature (from 900°C) EDP values close to those observed in the central one. The XRR obtained data seem to exclude, in the investigated temperature range, the presence of consistent inter-diffusion phenomena at the GDC/YSZ interface and give indication that, at least when dealing with clean crystalline interfaces, the optimized annealing temperature is around 900°C. This result is an important achievement when compared to what observed in PLD-deposited samples showing diffusion of yttrium in the GDC layers. Such a diffusion seems not to be present in our sputter deposited samples probably due to the different temperature conditions during the sample growth.

References

1. Santiso J, Burriel M (2011) Deposition and characterisation of epitaxial oxide thin films for SOFCs. *J Solid State Electrochem* 15: 985-1006.
2. Huang H, Nakamura M, Su P, Fasching R, Saito Y, et al. (2007) High-performance ultrathin solid oxide fuel cells for low-temperature operation. *J Electrochem Soc* 154: B20-B24.
3. Knibbe R, Hjelm J, Menon M, Pryds N, Søgaard M, et al. (2010) Cathode-electrolyte interfaces with CGO barrier layers in SOFC. *J Am Ceram Soc* 93: 2877-2883.
4. Barfod R, Hagen A, Ramousse S, Hendriksen PV, Mogensen M (2006) Break down of losses in thin electrolyte SOFCs. *Fuel Cells* 6: 141-145.
5. Yokokawa H, Sakai N, Horita T, Yamaji K, Brito ME, et al. (2008) Thermodynamic and kinetic considerations on degradations in solid oxide fuel cell cathodes. *J Alloys Compd* 452: 41-47.
6. Zhou XD, Scarfino B, Anderson HU (2004) Electrical conductivity and stability of Gd-doped ceria/Y-doped zirconia ceramics and thin films. *Solid State Ionics* 175: 19-22.
7. Wang CM, Azad S, Shutthanandan V, McCready DE, Peden CH, et al. (2005) Microstructure of ZrO₂-CeO₂ hetero-multi-layer films grown on YSZ substrate. *Acta mater* 53: 1921-1929.
8. Shi DQ, Ionescu M, McKinnon J, Dou SX (2001) Growth orientation and surface morphology of CeO₂ films deposited by PLD using different deposition atmospheres. *Phys C* 356: 304-310.
9. Wu F, Pavlovskaya A, Smith DJ, Culbertson RJ, Wilkens BJ, et al. (2008) Growth and structure of epitaxial CeO₂ films on yttria-stabilized ZrO₂. *Thin Solid Films* 516: 4908-4914.
10. Song K, Schmid H, Srot V, Gilardi E, Gregori G, et al. (2014) Cerium reduction at the interface between CeO₂ and Y₂O₃-stabilised ZrO₂ and implications for interfacial oxygen non-stoichiometry. *APL Mater* 2: 03214.
11. Kerman K, Lai BK, Ramanathan S (2012) Free standing oxide alloy electrolytes for low temperature thin film solid oxide fuel cells. *J Power Sources* 202: 120-125.
12. Jordan N, Assenmacher W, Uhlebruck S, Haanappel VAC, Buckremer HP, et al. (2008) Ce_{0.8}Gd_{0.2}O₂ Protecting Layers Manufactured by Physical Vapor Deposition for IT-SOFC. *Solid State Ionics* 179: 919-923.
13. Hara A, Hirata Y, Sameshima S, Matsunaga N, Horita T (2008) Grain size dependence of electrical properties of Gd-doped ceria. *J Ceram Soc Japan* 116: 291-297.
14. Sagar RUR, Galluzzi M, Wan C, Shehzad K, Navale ST, et al. (2017) Large, Linear, and Tunable Positive Magnetoresistance of Mechanically Stable Graphene Foam-Toward High-Performance Magnetic Field Sensors. *ACS App Mat Interface* 9: 1891-1898.
15. Sagar RUR, Saleemi AS, Shehzad K, Navale ST, Mane RS, et al. (2017) Non-magnetic thin films for magnetic field position sensor. *Sensors and Actuators: A* 254: 89-94.
16. Jiang SP, Wang W (2005) Novel structured mixed ionic and electronic conducting cathodes of solid oxide fuel cells. *Solid State Ionics* 176: 1351-1357.
17. Arndt B, Noei H, Keller TF, Muller P, Vonk V, et al. (2016) Structure and Stability of Gd-doped CeO₂ Thin Films on Ytria-Stabilized Zirconia. *Thin Solid Films* 603: 56-61.
18. Patterson AL (1939) The Scherrer Formula for X-Ray Particle Size Determination. *Phys. Rev.* 56: 978-982.
19. Cheng JG, Zha SW, Huang J, Liu XQ, Meng GY (2003) Sintering behavior and electrical conductivity of Ce_{0.9}Gd_{0.1}O_{1.95} powder prepared by the gel-casting process. *Mater Chem Phys* 78: 791-795.
20. Kim S, Merkle R, Maier J (2004) Oxygen nonstoichiometry of nanosized ceria powder. *Surf Sci* 549: 196-202.
21. Wang Y, Duncan K, Wachsman ED, Ebrahimi F (2007) The effect of oxygen vacancy concentration on the elastic modulus of fluorite-structured oxides. *Solid State Ionics* 178: 53-58.
22. Rupp JLM, Fabbri E, Marrocchelli D, Han JW, Chen D, et al. (2014) Scalable Oxygen-Ion Transport Kinetics in Metal-Oxide Films: Impact of Thermally Induced Lattice Compaction in Acceptor Doped Ceria Films. *Adv Funct Mater* 24: 1562-1574.
23. Yasaka M (2010) X-ray thin film measurement techniques. *Rigaku J* 26: 1-9.
24. Parratt LG (1954) Surface studies of solids by total reflection of x-rays. *Phys Rev* 95: 359-369.
25. Nevot L, Croce P (1980) Characterization of surfaces by grazing X-ray reflection—Application to study of polishing of some silicate-glasses. *Revue de Physique Appliquee* 15: 761-779.
26. www.genx.sourceforge.net/doc/faq.html
27. Badwal SPS, Fini D, Ciacchi FT, Munnings C, Kimpton JA, et al. (2013) Structural and microstructural stability of ceria-gadolinia electrolyte exposed to reducing environments of high temperature fuel cells. *J Mater Chem A* 1: 10768-10782.